International Core Journal of Engineering Volume 8 Issue 8, 2022
ISSN: 2414-1895 DOI: 10.6919/ICJE.202208_8(8).0100

Simulation Study on the Effect of Incident Velocity on Particle Erosion of Silicone Rubber Material

Yihao Wen*, Zhigao Xu, Jinjin Wang
Rocket Force University of Engineering, Xi'an Shannxi, 710025, China
*hgdwenyihao@163.com

Abstract

The numerical simulation model of particle erosion of silicone rubber thermal insulation material was established, and the effect of particle incident velocity on the erosion of silicone rubber thermal insulation material was studied, which provided a reference for particle erosion protection of solid rocket ramjet thermal insulation layer. Based on the ALE algorithm, the Johnson-Cook plastic material model and the Thermal-Isotropy-Phase-Change thermal material model, LS-DYNA was used to simulate the process of single particles impacting the molten layer and carbonized layer of silicone rubber thermal insulation materials, and the effect of incident velocity of particles on erosion patterns was studied. The results show that the numerical simulation model of particle erosion silicone rubber thermal insulation material established in this paper is relatively reliable. The surface regression rate of the char layer increases with the increase of the particle incident velocity as a quadratic function trend. The deformation, damage and regression of the surface of the char layer are mainly determined by the energy conversion during particle impact.

Keywords

Silicone Rubber Thermal Insulation Material; Particle Erosion; Char Layer; Molten Layer; Solid Rocket Ramjet.

1. Introduction

Silicone rubber thermal insulation material has the advantages of strong heat resistance, mechanical properties and oxidation resistance. It is an important material for the thermal insulation layer of the solid rocket ramjet combustion chamber, which has been widely valued by researchers [1]. During the high-speed maneuvering of the solid rocket ramjet missile, the two-phase products in the combustion chamber will locally aggregate under the action of centrifugal force, resulting in a high concentration of particles flowing with the high-temperature gas, which not only causes a strong mechanical erosion effect on the thermal insulation layer, but also increases the heat exchange between the thermal insulation material and the gas[2], aggravating the ablation damage of the inner wall, and even causes the engine casing to burn through and explode[3]. Therefore, it is very important to carry out research on particle erosion.

Previous scholars have carried out some researches on particle erosion of silicone rubber thermal insulation materials in high temperature jet environment. In 1993, Yang et al. [4] established a calculation model for ablation of thermal insulation materials, and divided the influencing factors of ablation of thermal insulation materials into two aspects: thermochemical ablation and mechanical erosion of particles. In 2006, Li et al. [5] studied the effect of particle erosion on EPDM thermal insulation materials through a small solid rocket ablation engine. The results show that the particle velocity was the main factor to aggravate the ablation of the thermal insulation layer, and the particle

ISSN: 2414-1895
DOI: 10.6919/ICJE.202208_8(8).0100

concentration had little effect on the ablation rate. In 2011, Zhang et al. [6] conducted a comparative test on the corrosion resistance of silicone rubber thermal insulation materials and EPDM thermal insulation materials under the condition of high concentration particle flow scouring. The results showed that the pyrolysis of the matrix generated gaseous or molten SiO2, which made the char layer of the silicone rubber insulation material loose and porous, resulting in a weaker corrosion resistance than the EPDM thermal insulation material. In 2017, Liu et al. [7] studied the ablation test characteristics of silicone rubber thermal insulation materials and EPDM thermal insulation materials under the condition of low-speed particle erosion. The results showed that the liquid SiO2 generated by the pyrolysis of the silicone rubber thermal insulation material matrix at low temperature and low velocity would penetrate into the surface of the thermal insulation material. Dense SiC was generated in the carbonized layer, which makes the particle erosion resistance of the silicone rubber insulation material stronger than that of the EPDM insulation material. The reason for the different conclusions of Zhang and Liu research is that the temperature and speed used in their experiments were different, but no scholars have come to a generally applicable conclusion since then.

To sum up, the current research on particle erosion of silicone rubber thermal insulation materials mainly relies on ablation experiments, lacking relevant theoretical and simulation models. Due to the disadvantages of high cost and poor repeatability in the ablation test, only the ablation law under specific test conditions can be obtained, and the specific process and influencing factors of the mechanical ablation of the meso-level particles on the silicone rubber thermal insulation material cannot be studied.

Therefore, this paper innovatively established a simulation model of single particle erosion of silicone rubber thermal insulation materials, and studies the influence of particle incident velocity on the mechanical erosion behavior of silicone rubber thermal insulation materials at the mesoscopic level. It could provide a new numerical simulation method for studying the particle erosion behavior and laws of silicone rubber thermal insulation materials, and provide a certain reference for particle protection of silicone rubber thermal insulation materials.

2. Numerical Methods

2.1 ALE Method

Under the high temperature jet environment, a molten layer of liquid phase will be formed on the surface of the silicone rubber thermal insulation material [1]. Therefore, the fluid-solid coupling method needs to be used in the numerical simulation of the process of particle erosion on the silicone rubber thermal insulation material. The Arbitratry Lagrangian Eulerian (ALE) method can not only prevent the material from being severely deformed and lead to the distortion of the Lagrange grid element and cause calculation errors, but also solve the problem that the Eulerian method is difficult to describe and capture the change of the structure boundary of the object, which is suitable for describing the flow solid coupling process. Therefore, this paper adopts the ALE method. Its governing equation is as follows:

Mass conservation equation:

$$\int_{\Omega}\left[\frac{\partial \rho(\chi,t)}{\partial t}+c_i\frac{\partial \rho}{\partial x_i}+\rho\frac{\partial v_i}{\partial x_i}\right]\mathrm{d}\Omega=0 \tag{1}$$

Momentum conservation equation:

$$\rho\left[\frac{\partial v_i(\chi,t)}{\partial t}+c_j\frac{\partial v_i}{\partial x_j}\right]=\frac{\partial \sigma_{ij}}{\partial x_j}+\rho b_i \tag{2}$$

ISSN: 2414-1895 DOI: 10.6919/ICJE.202208_8(8).0100

Energy conservation equation:

$$\rho\left[\frac{\partial E(\chi,t)}{\partial t}+\frac{\partial E}{\partial x_i}c_i\right]=\frac{\partial \sigma_{ij}v_i}{\partial x_j}+b_i v_i+\frac{\partial\left[k_{ij}\frac{\partial\theta}{\partial x_j}\right]}{\partial x_i}+\rho s \tag{3}$$

Boundary conditions:

$$f_i(\chi,t)=n_j(\chi,t)\sigma_{ji}(\chi,t)\Big|_{\Gamma_f} \tag{4}$$

$$q_i(\chi,t)=-k_{ij}(\theta,\chi,t)\frac{\partial\theta(\chi,t)}{\partial x_j}+k_i(\theta,t)(\theta-\theta_0)\Big|_{\Gamma_q} \tag{5}$$

$$\begin{cases} u_i(\chi,t)=\bar{u}(\chi,t)\Big|_{\Gamma_{u_i}} \\ \theta(\chi,t)=\bar{\theta}(\chi,t)\Big|_{\Gamma_{u\theta}} \end{cases} \tag{6}$$

where, $c=v-\hat{v}$ is the grid transfer velocity, E is the internal energy of the substrate, k is the convective heat transfer coefficient, θ is the temperature, i and j is the row and column coordinates of the matrix, respectively, Equation (4) represents the boundary condition of the force, and Equation (5) represents the boundary condition of heat flow, and equation (6) represents the displacement boundary.

2.2 Finite Element Impact Model

When the solid rocket ramjet is working, the gas temperature can reach more than 2000 K, the gas velocity at the nozzle can reach more than 1000 m/s, the particle temperature can reach more than 1000 K, and the particle speed can reach more than 400 m/s. After ablation of the silicone rubber thermal insulation material, there will be obvious delamination, from the outside to the inside, the molten layer, the char layer, the pyrolysis layer and the matrix layer, and the particle erosion mainly occurs between the molten layer and the carbonized layer [8], in order to simplify the calculation, the impacted matrix is mainly the molten layer and the char layer. The particles are selected from boron particles that are commonly used in ramjets, which usually appear as B2O3 particles in the engine gas environment [9, 10].

A three-dimensional finite element impact model of the particles and the matrix was established as shown in Figure 3. In order to simplify the calculation, the particle diameter is taken as the average diameter of 15 μm [11], the matrix is composed of the molten layer and the carbonized layer, the thickness of the molten layer was taken as 10 μm, and the thickness of the char layer was taken as 100 μm. The length and width of the matrix are larger than those of the particles 4 times the diameter, the influence of the matrix boundary node on the deformation area of the matrix center during the particle impact process can be ignored [12], the incident angle is 30°, and the erosion conditions were calculated under six particle incident velocities, including 250 m/s, 300 m /s, 350 m/s, 400 m/s, 450 m/s and 500 m/s.

Volume 8 Issue 8, 2022
DOI: 10.6919/ICJE.202208_8(8).0100

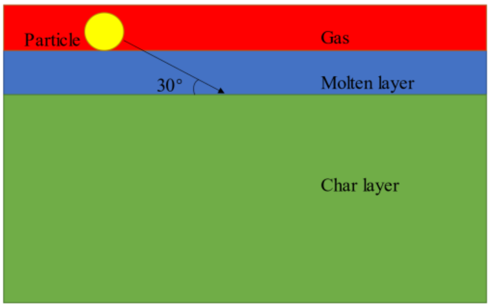

Figure 1. The finite element impact model

2.3 Material Model

The Johnson-Cook plasticity model [13] is often used to describe the strength limit and failure process of metal materials in large strain, high strain rate, and high temperature environments, and can be used to describe the behavior of B2O3 particles hitting a molten layer with high viscosity. Therefore, the particles adopt the Johnson-Cook plasticity model. The specific expression of the Johnson-Cook plasticity model is as follows:

$$\tau=\left[A+B\left(\varepsilon_{\mathrm{p}}\right)^{n}\right]\left(1+C\ln\dot{\varepsilon}^{*}\right)\left[1-\left(T^{*}\right)^{m}\right] \tag{7}$$

$$\dot{\varepsilon}^{*}=\frac{\dot{\varepsilon}_{\mathrm{p}}}{\dot{\varepsilon}_{0}} \tag{8}$$

$$T^{*}=\frac{T-T_{\mathrm{r}}}{T_{\mathrm{m}}-T_{\mathrm{r}}} \tag{9}$$

where, τ is the yield stress of the material, A is the initial yield stress, B is the strain hardening modulus, C is the strain rate hardening modulus, ε_{p} is the equivalent plastic strain of the material, $\dot{\varepsilon}_{\mathrm{p}}$ is the equivalent plastic strain rate of the material, and $\dot{\varepsilon}_{0}$ is the material refers to the equivalent plastic strain rate, T is the material temperature, T_{r} is the ambient temperature, T_{m} is the material melting temperature, n is the strain strengthening index, and m is the temperature softening index.

The Plastic kinematic model comprehensively considers isotropic hardening, kinematic hardening or a combination of the two, and has the advantages of considering the influence of strain rate and high computational efficiency, and can describe most of the hardening collision problems, which is appropriated to describe the char layer material. Its expression is as follows:

$$\sigma_{y}=\left[1+\left(\frac{\dot{\varepsilon}}{C}\right)^{\frac{1}{p}}\right]\left(\sigma_{0}+\beta E_{\mathrm{p}}\varepsilon_{\mathrm{eff}}^{\mathrm{p}}\right) \tag{10}$$

$$E_{p}=\frac{E_{\mathrm{t}}E}{E-E_{\mathrm{t}}} \tag{11}$$

where, σ_{y} is the yield strength of the material, $\dot{\varepsilon}$ is the strain rate of the material, σ_{0} is the initial yield strength of the material, β is the control coefficient, E is the elastic modulus, Et is the tangent

ISSN: 2414-1895
DOI: 10.6919/ICJE.202208_8(8).0100

modulus, $\varepsilon_{\mathrm{eff}}^{\mathrm{p}}$ is the effective plastic strain of the material, C, p are parameters related to strain rate in the Cowper-Symonds model.

The NULL model was used for the gas and molten layer, and the Thermal-Isotropy-Phase-Change thermal material model was selected for the thermal material model of particles and the substrate. The parameters used in the calculation were all from the LS-DYNA material library and related literature [14], as shown in Table 1.

Table 1. Particle and substrate parameters

Material parameters	Particle	Melting layer	Char layer
Density /kg m^{-3}	2460	2160	2000
Young's modulus /GPa	0.132	-	4.5
Shear modulus /GPa	77	-	-
Poisson's ratio	0.33	-	0.375
Static yield strength /GPa	0.102	-	-
Static hardening modulus /GPa	0.050	-	-
Strain rate hardening modulus	0.01	-	-
Thermal softening index	0.859	-	-
Strain rate hardening index	0.197	-	-
Reference temperature /K	293	-	-
Melting temperature /K	893	-	-
Heat capacity/ ($J \cdot kg^{-1}$ K^{-1})	486	4200	1700
Viscosity coefficient / (kg m^{-1} s^{-1})	-	8.684×10^{-4}	-
Thermal conductivity/ ($W \cdot m^{-1} \cdot K^{-1}$)	237	0.59	0.21

2.4 Meshing

Figure 2 shows the meshing of the computational area. Because the mesh size has a great influence on the heat conduction and deformation between the particles and the molten layer and the char layer [15], the mesh was refined to ensure the calculation accuracy, and the mesh size between the particles and the matrix is 0.5 μm. Full constraints were imposed on the bottom surface of the carbonized layer, symmetry constraints was imposed on the symmetry plane, and non-reflection boundary conditions were imposed on the sides of the substrate in each layer, and the rest of the surfaces were set as free states. The contact algorithm between particle and matrix adopts AUTO-Surface to Surface method.

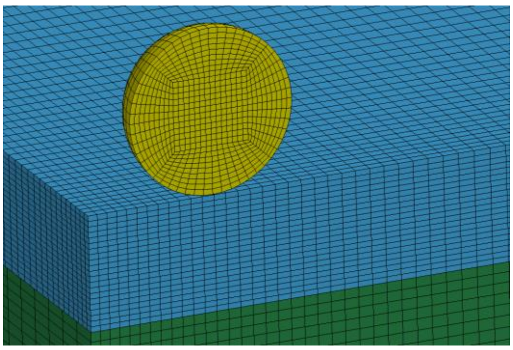

Figure 2. Meshing

3. Results and Discussion

3.1 Influence of Particle Incident Velocity on Surface Regression Distance of Char Layer

The molten layer can play a certain role in insulating heat flow. The char layer plays an important role in maintaining the structural integrity of silicone rubber thermal insulation materials. The erosion of particles to silicone rubber insulation is mainly reflected in mechanical erosion, that is, high-speed particle impact destroys the molten layer, accelerates the regression of the char layer, and then destroys the structural integrity of the silicone rubber insulation. Therefore, it is necessary to study the law of surface retreat of carbonized layer.

Figure 3 shows the comparison of the surface deformation of the silicone rubber thermal insulation material caused by the particle impact at 0.45 μs with different particle incident velocities. It can be seen from the figure that when the particles hit the molten layer, they were greatly deformed and became flat, and the side with the same incident direction as the particle (the right side in the figure) had a more obvious flattening trend. The molten layer appeared hemispherical impact craters. The slope of the impact crater is gentler on the same side as the incident direction of the particles (the right side in the figure), and the left side of the impact crater is formed due to the shearing action of the particles on the molten layer, and the morphology of the right side of the impact crater due to the extrusion of the particles on the molten layer. However, the surface deformation of the char layer is relatively small. With the increase of particle incident velocity, the depth and area of the crater in the molten layer gradually increased, but the increase rate of the crater depth was smaller than that of the crater diameter, indicating that the particles with higher incident velocity had a greater degree of slip on the surface of the molten layer. The regression distance of the surface of the char layer gradually increases, and after v=400 m/s, there are identifiable depressions on the surface of the char layers.

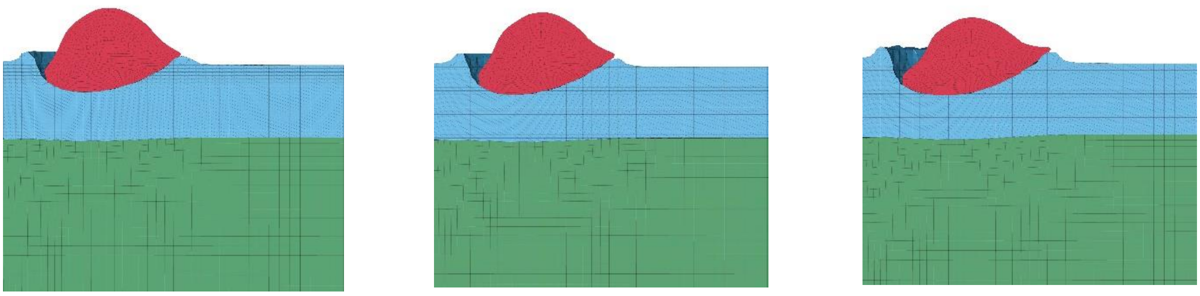

a. v=250 m/s b. v=300 m/s c. v=350 m/s

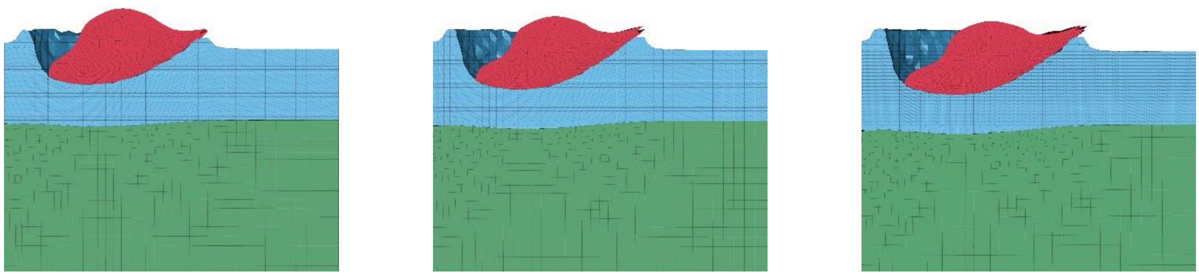

d. v=400 m/s e. v=450 m/s f. v=500m/s

Figure 3. Deformation comparison of molten layer and carbonized layer under different particle incident velocities

ISSN: 2414-1895
DOI: 10.6919/ICJE.202208_8(8).0100

The nodes with the largest regression distance on the surface of the char layer were selected in each case under different particle incident velocities, and their regression distance were compared, as shown in Figure 4. It can be seen from the figure that at the same time, as the particle incident velocity gradually increases, the regression distance of the char layer caused by particle erosion increases; however, this increasing effect gradually becomes less obvious as the particle incident velocity increases. The reason is that with the velocity increases, the slip effect of particles on the surface of the molten layer is enhanced, a larger proportion of the kinetic energy is absorbed by the molten layer, and the regression distance increase rate of the char layer becomes slower.

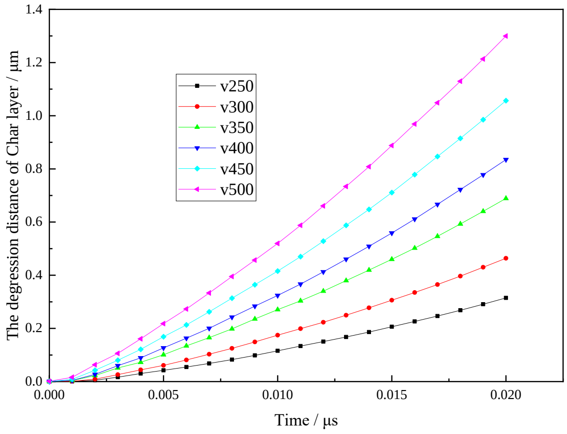

Figure 4. Comparison of the char layer regression rate under different particle incident velocities

Through nonlinear curve fitting, the relationship between the particle incident velocity and the surface regression distance of the char layer under the conditions of this paper can be obtained, as shown in Figure 5, and its specific expression is shown in Equation (12).

$$l = F(v_0) = 1.78074 \times 10^{-5} v_0^2 - 0.01026 v_0 + 3.20558 \tag{12}$$

According to Figure 5 and Equation (12), it can be seen that the particle incident velocity has a significant effect on the surface regression distance of the char layer. With the increase of the particle incident velocity, the regression distance of the char layer gradually increases, and the overall trend increases as a quadratic function, which is the same as the increase in kinetic energy. Therefore, it is speculated that the regression distance of the char layer is closely related to the conversion of kinetic energy in the process of particles hitting the silicone rubber insulation material.

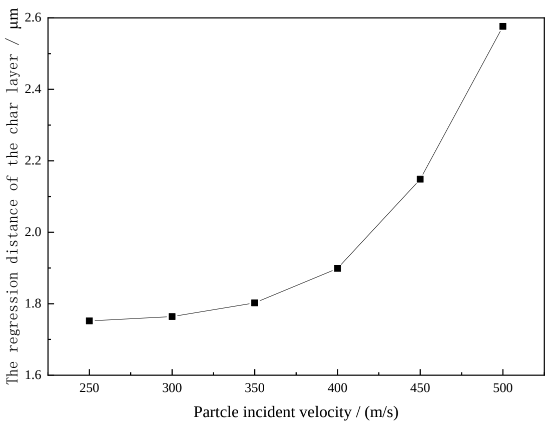

Figure 5. The relationship between the regression distance of the char layer and the particle incident velocity

Volume 8 Issue 8, 2022
DOI: 10.6919/ICJE.202208_8(8).0100

3.2 Influence of Particle Incident Velocity on Particle Erosion Energy Conversion

In the process of particles eroding the silicone rubber insulation material, the kinetic energy of the particles is converted into the internal energy of the molten layer, the internal energy of the char layer, and a part of it is dissipated in the form of heat. The law of energy conversion in this process can reflect to the reasons for the deformation of the molten layer and char layer of the silicone rubber thermal insulation material.

Figure 6 shows the time-dependent curves of particle kinetic energy at different incident velocities. It can be seen from the figure that the kinetic energy loss rates of particles with different incident velocities are different. The higher the velocity, the faster the kinetic energy loss rate of the particles. The kinetic energy at the termination time of particle impact also has obvious variation rules. The kinetic energy at the termination time of particle impact under different incident velocities was extracted, and the termination kinetic energy curve was obtained by nonlinear curve fitting. It can be seen from this curve that when the particle incident velocity is low, as the particle incident velocity increases, the impact duration of the particle decreases rapidly, but the kinetic energy increases slowly at the termination time; when the particle incident velocity is high, as the particle incident velocity increases, with the further increase of the speed, the duration of the particle impact is basically unchanged, but the kinetic energy of the particle increases rapidly at the time of termination. Combined with the actual process of particle impacting the silicon rubber thermal insulation material, it's because when the particle incident velocity is low, the particle has sufficient time to deform and break. During this process, the kinetic energy of the particle can be fully converted into the internal energy of the molten layer and the internal energy of the carbonized layer. and so on, so the particle termination kinetic energy does not increase with the increase of the initial kinetic energy trend; when the particle incident velocity is large, the deformation and fragmentation time of the particle is short, and the particle kinetic energy is dissipated in the form of heat during the particle fragmentation process, so the final kinetic energy of the particle increases in the same trend as the initial kinetic energy, which increases as a quadratic function with increasing velocity.

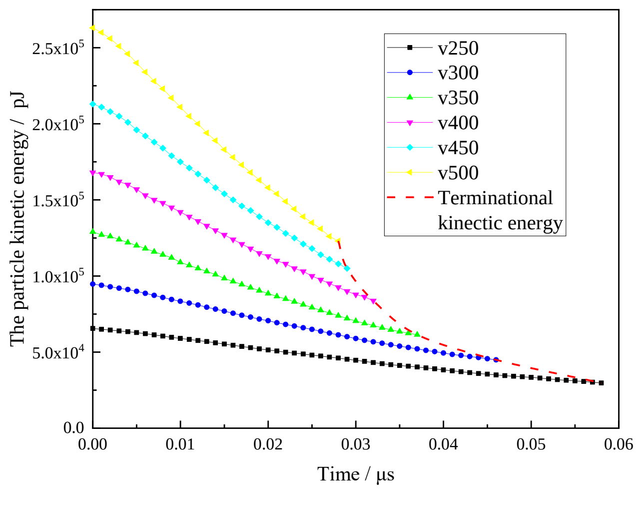

Figure 6. Comparison of particle kinetic energy loss

Figure 7 shows the comparison of the internal energy increment of the char layer caused by particle erosion at different incident velocities. It can be seen from the figure that due to the short particle erosion process, the relationship between the internal energy increment of the char layer and time under different particle incident velocities can be regarded as linear, and the internal energy increment-time curve of the char layer can be approximately regarded as a straight line. The slopes of these straight lines increase as the incident velocity increases, but this increase is uniform, and the slope increases at the same rate when the particle incident velocity is larger or smaller. Figure 8 shows

 Volume 8 Issue 8, 2022
DOI: 10.6919/ICJE.202208_8(8).0100

the comparison of the internal energy increment of the molten layer caused by particle erosion at different incident velocities. It can be seen from the figure that at a certain incident velocity, the growth rate of the internal energy of the molten layer gradually decreases. This phenomenon is more obvious when the particle incident velocity is low (as 250 m/s or 300 m/s). This is because as the particles hit the molten layer, the particle velocity gradually decreases, the friction and hysteresis of the molten layer are weakened, and the rate at which the kinetic energy of the particles is converted into the internal energy of the molten layer decreases. When the particle incident velocity is low, the impact duration is longer, so this phenomenon is more obvious.

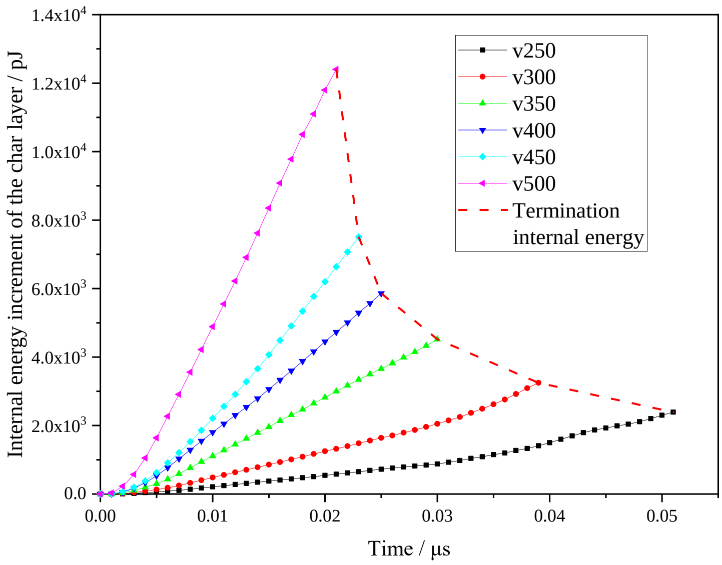

Figure 7. Comparison of the increase in the internal energy of the char layer

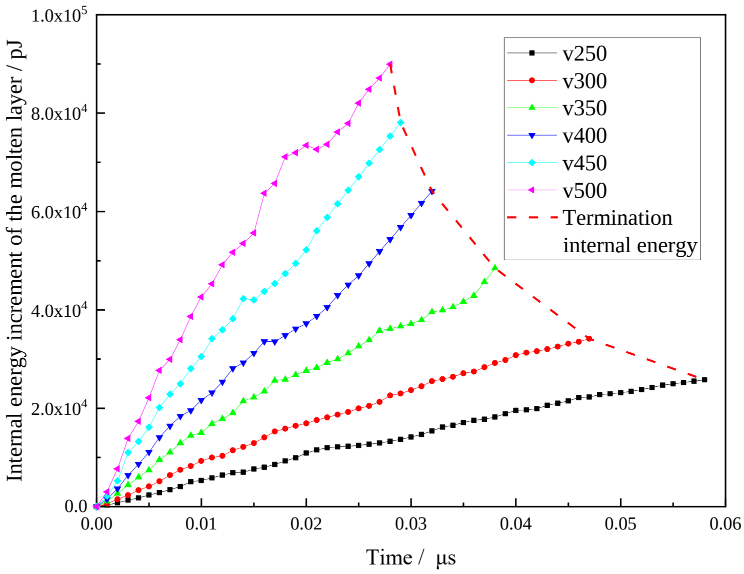

Figure 8. Comparison of the increase in the internal energy of the molten layer

In order to reflect the energy conversion relationship in the process of particle erosion of the silicone rubber thermal insulation material, the energy curves at the termination time in Fig. 6, Fig. 7 and Fig. 8 were extracted and concentrated on the comparative analysis in Fig. 9. It can be seen from the figure that with the increase of the particle incident velocity, the kinetic energy of the particles at the termination time increases faster than that of the internal energy of the molten layer and the internal energy of the char layer, indicating that the heat dissipation in the process of the particles hitting the silicone rubber insulation material gradually increases, and the proportion of particle kinetic energy converted into the internal energy of the molten layer and the char layer is smaller. Therefore, the friction, buffering and energy absorption of the molten layer and the char layer are weakened. However, due to the relatively short impact time of the particles, on the whole, the variation trend of the internal energy of the char layer is approximately the same as the variation trend of the particle kinetic energy. Therefore, the variation trend of the char layer internal energy with the particle incident velocity also shows a quadratic function growth trend.

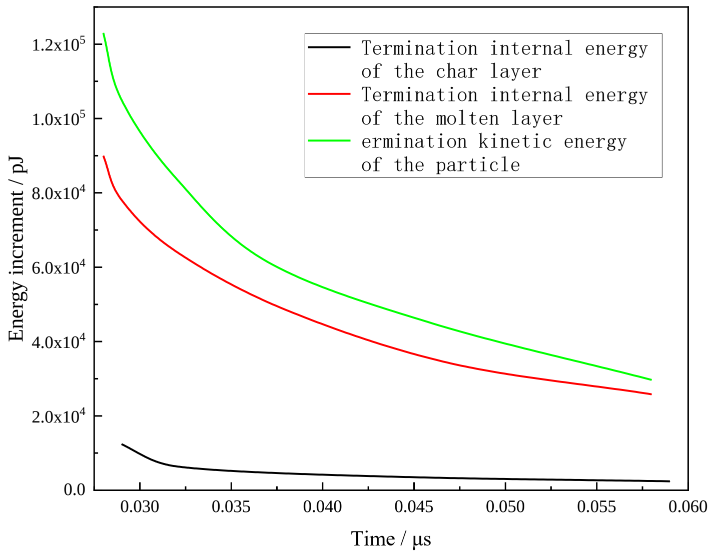

Figure 9. Comparison of termination energy curves of particle, molten layer and char layer

As Fig. 10, the calculation results of the regression distance of the char layer under different particle incident velocities were compared with the calculation results of the internal energy increment of the char layer. It can be seen that the change trend of the two is similar, so the inference of the reason for the regression distance is correct, and the regression distance of the char layer is directly related to the conversion between the particle kinetic energy and the char layer internal energy.

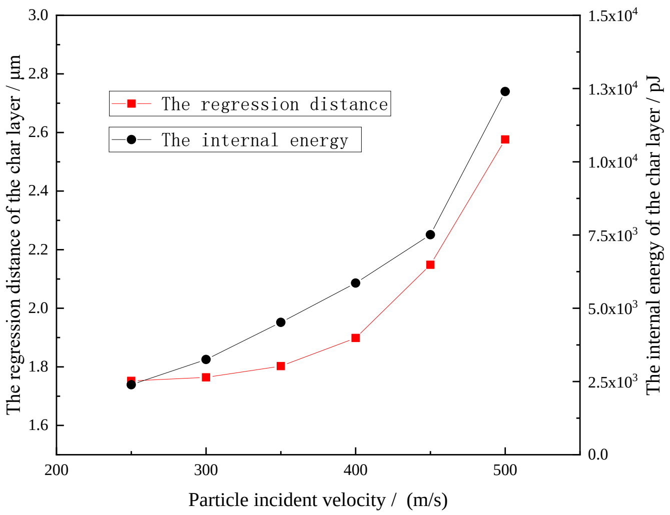

Figure 10. The relationship between the regression distance and the internal energy increment of the char layer

ISSN: 2414-1895 DOI: 10.6919/ICJE.202208_8(8).0100

4. Conclusion

In this paper, based on the ALE method, a numerical simulation model of single particle erosion on silicone rubber thermal insulation materials was established by LS-DYNA software, the process of single particle impacting the molten layer and the char layer was simulated, and the effect of particle incident velocity on the erosion law was studied. The following conclusions can be drawn:

(1) The numerical simulation model of particle erosion silicone rubber thermal insulation material established in this paper is relatively reliable. Under this paper's calculation conditions, the surface regression distance of the char layer increases as a quadratic function with the increase of the particle incident velocity.

(2) As the increase of particle incident velocity, the heat dissipation in the process of the particles hitting the silicone rubber insulation material gradually increases, and the proportion of particle energy converted into the internal energy of the molten layer and the char layer is smaller. And the friction, buffering and energy absorption of the molten layer and the char layer are weakened.

(3) The regression distance of the char layer is directly related to the variation of the char layer internal energy.

References

[1] Li J, Guo M.F., Liu Y, et.al. Review on Ablation Research of Insulation Materials for Solid Rocket Motors[J], Journal of Astronautics, 40(10) (2019) 11.

[2] Lou Y.C. Experimental Study of Insulation Ablation Eroded by High-Temperature and Dense Two-Phase Flow[D], Northwestern Polytechnical University, 2005.

[3] Melia, Peter, Flow and Ablation Patterns in Titan IV SRM aft Closures[C], 31st Joint Propulsion Conference and Exhibit, 1995.

[4] B.C. Yang, F.B. Cheung, J.H. Koo, Numerical Investigation of Thermo-chemical and Mechanical Erosion of Ablative Materials[C], 29th Joint Propulsion Conference and Exhibit, 1993.

[5] Li J, Liu Y, Lou Y.C. et.al. Experimental investigation for the influence of Particle on Insulation Erosion[J], Journal of Propulsion Technology, 27(1) (2006) 4.

[6] Zhang S.M., Hu C.B., Xia S.Y., et.al. Real-time Ablation Measurements on Erosion of Silicon Rubber and EPDM Material by Highly Concentrated Particles[J], Journal of Propulsion Technology, 32(2) (2011) 5.

[7] Liu Y, Guan Y.W., Wu Y.F., et.al. Experimental Investigation on Ablation Characteristic of Silicon Rubber Insulator under Particle Erosion Condition[J], Journal of Propulsion Technology, 38(1) (2017) 8.

[8] Liu X, Guo Y.J., Liu W, et.al. Numerical Simulation Research on Three-Dimensional Ablative Thermal Response of Charring Ablators[J], Journal of Astronautics, 37(9) (2016) 7.

[9] W. Jung, S. Baek, J. Park, S. Kwon, Combustion Characteristics of Ramjet Fuel Grains with Boron and Aluminum Additives [J], Journal of Propulsion & Power (2018) 1-10.

[10] T. Mitani, M. Izumikawa, Combustion Efficiencies of Aluminum and Boron in Solid Propellants[J], Journal of Spacecraft & Rockets 28(1) (2012) 79-84.

[11] Wang J.J., Zha B.L., Zhang Y, et.al. Study of Ablation Properties of Silicone Rubber Composite under Particle Erosion[J], Acta Armamentarii, 40(4) (2019) 9.

[12] H. Assadi, F. G. Rtner, T. Stoltenhoff, H. Kreye, Bonding mechanism in cold gas spraying[J], Acta Materialia, 51(15) (2003) 4379-4394.

[13] G.R. Johnson, W.H. Cook, A constitutive model and data for metals subjected to large strains, high strain rates and high temperatures, Engineering Fracture Mechanics 21 (1983) 541-548.

[14] Jiang G.Q., Liu L.Y. Heat Transfor of Hypersonic Gas and Ablation Thermal Protection [M], National Defence Industry Press, Beijing, 2003.

[15] D.Y. Tzou, A Unified Field Approach for Heat Conduction From Macro- to Micro-Scales[J], Journal of Heat Transfer, 117(1) (1995) 8-16.